



Project no. TIP5-CT-2006-031415

INNOTRACK

Integrated Project (IP)

Thematic Priority 6: Sustainable Development, Global Change and Ecosystems

D4.1.2 Interim Rail Degradation Algorithms

Due date of deliverable: 2008/02/29

Actual submission date: 2008/05/02

Start date of project: 1 September 2006

Duration: 36 months

Organisation Name of lead contractor for this deliverable: Corus and VAS

Final

Project co-funded by the European Commission within the Sixth Framework Programme (2002-2006)		
Dissemination Level		
PU	Public	X
PP	Restricted to other programme participants (including the Commission Services)	
RE	Restricted to a group specified by the consortium (including the Commission Services)	
CO	Confidential, only for members of the consortium (including the Commission Services)	

Table of Contents

List of figures and tables	2
Glossary	3
1. Executive Summary	4
2. Introduction	5
3. Rail Degradation Mechanisms	6
3.1 Loss of Rail Profile	6
3.2 Rolling Contact Fatigue (RCF)	7
3.3 Increased Rail Breakage Risk	8
4. Data Processing	10
4.1 Received Data	10
4.1.1 <i>Corus</i>	10
4.1.2 <i>Voestalpine (VAS)</i>	10
4.2 Limitations of Data	10
4.3 Combined Data	12
4.3.1 <i>Wear Calculations</i>	12
4.3.2 <i>Rolling Contact Fatigue (RCF) Calculations</i>	14
5. Rail Degradation	15
5.1 Wear	15
5.2 Rolling Contact Fatigue (RCF)	20
6. A Basis for a General Degradation Approach	24
6.1 Motivation	24
6.2 Basic Conventions	24
6.3 Calculation	25
6.3.1 <i>Input parameter</i>	25
6.3.2 <i>Resulting Loads</i>	25
6.3.3 <i>Resulting stresses</i>	26
6.3.4 <i>Interpretation of interim results</i>	28
6.3.5 <i>Intended further work</i>	29
7. Conclusions	30
8. Bibliography	31

List of figures and tables

Figure 1 - A Range of Rail Profiles Encountered on Railways	6
Figure 2 - RCF Cracks.....	7
Figure 3 - Example of a Sub-surface Initiated RCF Crack	8
Figure 4 - Rail breakage from a fatigue crack initiating at a corrosion pit	9
Figure 5 – 45° Wear against traffic – Regression Analysis	13
Figure 6 – 45° Wear against traffic – Maximum Wear Rate Analysis	13
Figure 7 - Schematic of crack growth rates	14
Figure 8 – 45° Wear of grade 220 rails - nominal cant.....	15
Figure 9 – 45° Wear of non-220 grade rails	16
Figure 10 - Affect of rail hardness on 45° wear of curves with radius less than 700m	17
Figure 11 - log wear rate against log radius, R260 and R350HT	17
Figure 12 - Wear rate against log radius, 220	18
Figure 13 - Vertical wear of grade 220 rails – cant deficiency.....	19
Figure 14 - Vertical wear of non 220 grade rails – cant deficiency	20
Figure 15 - Maximum crack depth growth rate since installation for all rail grades.....	21
Figure 16 - Maximum surface crack length growth rate since installation for all rail grades.....	21
Figure 17 - Period to Initiation of RCF cracks	22
Figure 18 - Distribution of radius [1000m] for segmented track with RCF defects.....	22
Figure 19 - Schematic of RCF and wear	24
Figure 20 - Coordinate system for modelling.....	25
Table 1 - Calculation of stresses for three test sites	28

Glossary

Abbreviation/acronym	Description
RCF	Rolling contact fatigue
IM's	Infrastructure Managers – i.e. the railway partners involved in the project
MGT	Million Gross Tonnes
MGTPA	A measure of traffic in units of million gross tonnes per annum
PTI	period to initiation
GC	Gauge corner
RS	Running Surface
W	Depth of wear

1. Executive Summary

Railways and rail manufacturers have collected large amounts of data on the degradation of rail over the years. This has given invaluable information on the performance of different rail grades in service. This data is being collected together in a database with the results reported in D4.1.1. This deliverable, reports on an initial analysis of this data aimed at deriving algorithms for the degradation of rails as a function of track geometry, rail grade and loading conditions. The derived algorithms will then be used to establish definitive guidelines for the selection of rail grades to maximise the expected life for the various duty conditions.

The analysis has shown that wear is the key degradation mechanism of rail for tight curves of less than 700m while rolling contact fatigue is a major problem for curves of intermediate radii. However, since maintenance of rail profile is also a key requirement for the management of RCF, understanding of wear behaviour for other track characteristics is also considered to be important. The initial analysis has demonstrated that this is a non-trivial problem because of the wide range of variables that are present within the collected data, further problems also include the lack of information on certain parameters that are important to the performance of rail in track. Although some clear trends have become apparent from the initial analysis, it has also revealed where further analysis is required and this will be reported in a further deliverable.

2. Introduction

A large selection of individual sites has been monitored by the two rail manufacturers, Corus and voestalpine, in partnership with the railway infrastructure managers. The aim of this monitoring has been to observe the performance of different rail steels under normal traffic conditions. A summary of the site characteristics is reported in the accompanying deliverable D4.1.1. This interim report details the work that is being carried out in work package WP4.1 to predict rail degradation and eventually to derive rail degradation algorithms that can be used to give guidance on rail grade selection (D4.1.3).

This deliverable details the data analysis that has been carried out to give empirical degradation rates of the rail as a function of track geometry and loading conditions for individual rail steels. Data collection has been led by the rail manufacturers and has therefore concentrated on the rails. Other supporting information that is not essential to compare the performance of rail grades on an individual site, but would allow a more comprehensive analysis of the data to be carried out has therefore not been recorded. The final version of this deliverable, due in month 36, would therefore be more comprehensive if this information could be made available by the Infrastructure Managers (IM's). Any other data from monitored sites that any partner in the project could make available would also improve the range of sites increasing the accuracy of the algorithms.

Initial analysis has been carried out using the data currently available. This has resulted in trends in the data being identified but no mathematical algorithms have currently been derived. A full analysis of the data taking into account all possible factors will therefore be prepared for the final version of the deliverable.

3. Rail Degradation Mechanisms

The key degradation mechanisms that limit the serviceable/operational life of rail are [1]:

- Loss of rail profile
 - Vertical and Side Wear
 - Corrugation
- Rolling Contact Fatigue (RCF)

The different degradation mechanism can be combated by different or a combination of material properties, a number of rail steel grades have been developed and are available to the industry with a range of different properties. The main deliverable of WP4.1 is a recommendation of the appropriate rail grade for different sections of track, this will take into account the different degradation mechanisms. However, it must be emphasised that rail degradation is the result of the whole system and hence rail metallurgy cannot be addressed independently. Optimisation of other aspects of the systems design and operation need to be taken into consideration in parallel. Thus any reduction in the stress levels within the contact patch brought about by optimisation of rail wheel profile is not only beneficial but provides synergistic benefits when combined with improved rail metallurgy.

3.1 Loss of Rail Profile

The loss of rail profile caused by wear and/or plastic deformation is one of the causes of increased frequency of maintenance or even of premature replacement of rail in track. The loss of profile includes both vertical and side wear of rails through the action of wheels on them and premature replacement is particularly true for tight radius curves because of high side wear even though vertical wear is well within permissible limits. Some examples of profiles from a range of locations are shown in Figure 1 but they do not represent similar accumulated tonnages carried. In view of the minor differences in profile that affect vehicles dynamic behaviour, it is interesting to note that quite significant change to profile can be tolerated over the life of the rail.

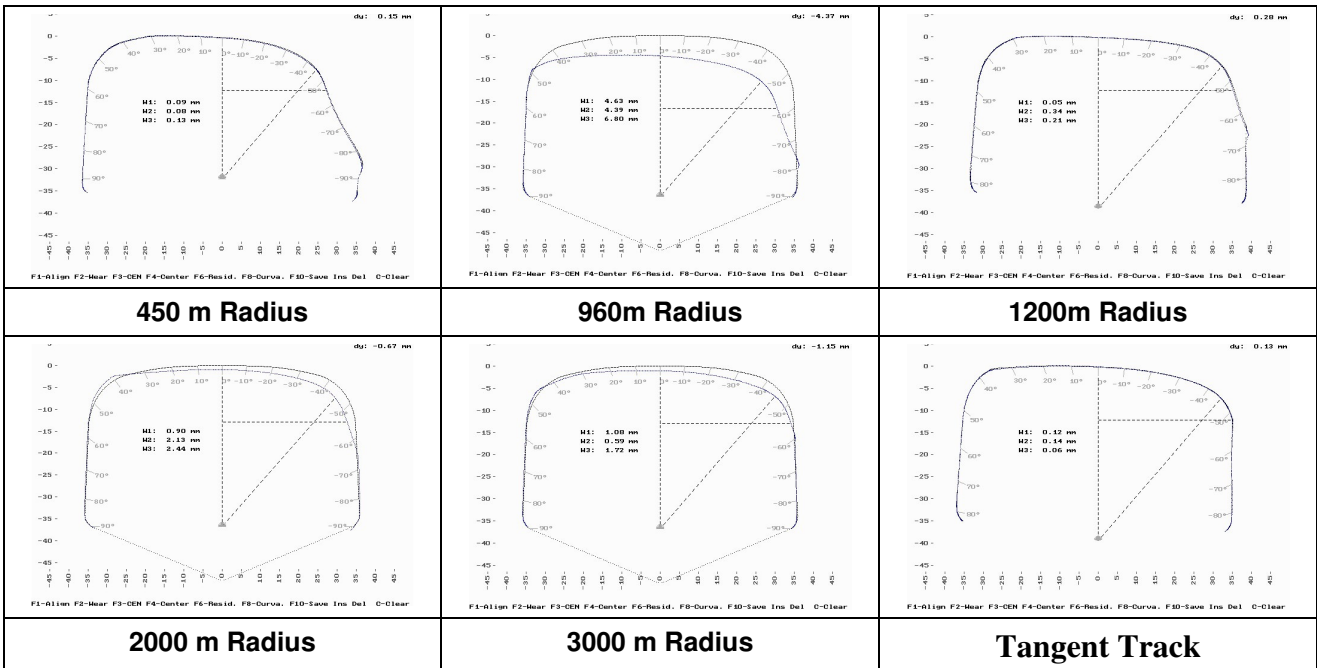


Figure 1 - A Range of Rail Profiles Encountered on Railways

Clearly, the ability to maintain the optimum rail profile for the different contact conditions for as long as possible is highly desirable, hence the development and use of steels that minimise the loss of transverse profile.

The occurrence of corrugations could also be regarded as loss of rail profile in the longitudinal direction particularly since it is not categorically established whether corrugation is a result of differential plastic deformation or differential wear or both. Although this statement may be seen in some circles as contentious, recent work involving the study of microstructural deformation, using electron back scatter diffraction techniques, is quite revealing and will be reported within a deliverable from WP4.3.

The material property parameters contributing to the control of both these issues are:

- Proof strength
- Wear resistance which itself shows a strong dependence on hardness

3.2 Rolling Contact Fatigue (RCF)

Rails are subjected to cyclic loading in service, the stress range and the magnitude of stresses being dependent on a range of variables including the rail and wheel profile, the contact patch position and size, and the dynamic track forces from the vehicle. Consequently, the phenomenon of fatigue becomes of critical importance to longevity of rails. Although fatigue in rails manifests itself in many ways, the two major classifications of rolling contact fatigue (RCF) are "squats" and "head checks" (Figure 2) both of which can be associated with early propagation of surface or near surface initiated rolling contact fatigue cracks. The hive of research and development activity in both the UK and other European Railways on RCF since the Hatfield derailment is a clear indication of the importance of this issue for safety and the longevity of rails.



Figure 2 - RCF Cracks

The stages in the life of surface initiated RCF cracks are:

- Crack initiation
- Shallow angle crack
- Turn down and growth of turned down cracks. In some cases, cracks can turn upwards and/or merge with neighbouring cracks to cause "shelling" which renders the rail un-inspectable and hence enforcing replacement.

RCF cracks can also be initiated sub-surface, an example of which is shown in Figure 3. Often such defects or breaks can be classified as "Tache Ovale" and attributed to presence of inclusions. Although, modern steelmaking practice has eliminated failures associated with inclusions, sub-surface fatigue cracks can still be initiated because of inappropriate contact conditions giving rise to high sub-surface shear stresses.

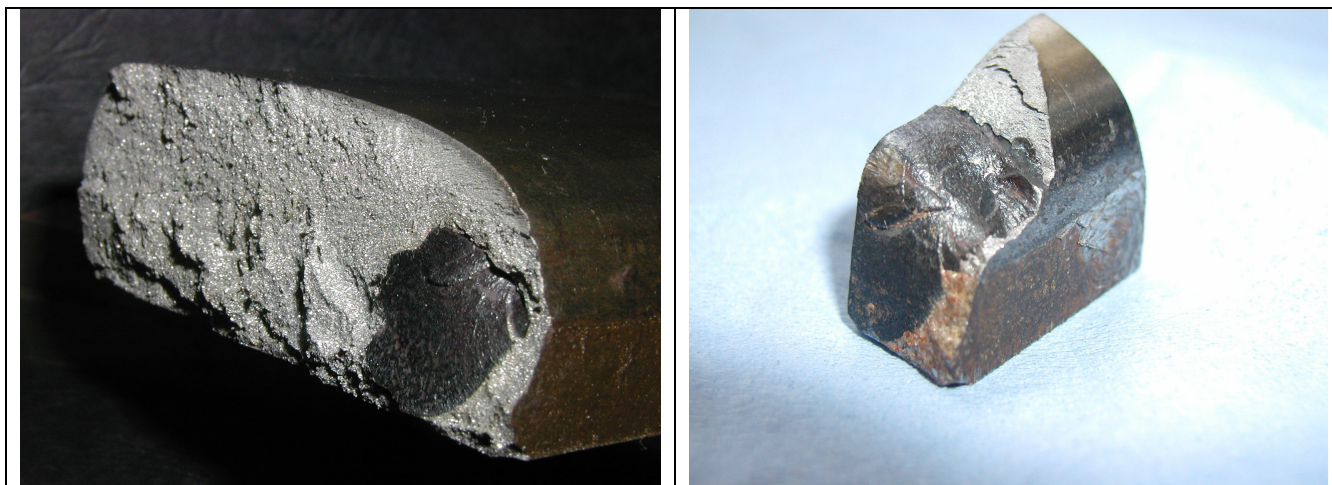


Figure 3 - Example of a Sub-surface Initiated RCF Crack

The resistance to RCF of rail steels does not feature in any rail steel specification. However, in view of the growing acknowledgement by most railways that RCF is a key cause for rail life curtailment, it is essential to establish a measure of RCF resistance in terms of:

- Period or cycles to initiation
- Growth rate of cracks during shallow angle stage
- Growth rate of cracks following turn down governed primarily by standard fracture mechanics principles

3.3 Increased Rail Breakage Risk

Rail breaks and defectives, Figure 4, form the third category of rail degradation and fracture mechanics principles clearly demonstrate the importance of key material properties required to make rail steels more tolerant of in-service conditions. Rail breaks result from a number of causes including:

- Rail foot corrosion
- Failure at rail ends, including from bolt holes
- Failure of welds
- Internal defects

Failures from the various manifestations of RCF also pose an increased risk as indicated in the previous section.

The material properties relevant to the assessment of the risk of rail breakages are:

- Fracture toughness
- Impact properties
- Fatigue crack growth rate
- Full rail section bending fatigue strength
- Defect size tolerance
- Level of residual stress in various parts of the rails



Figure 4 - Rail breakage from a fatigue crack initiating at a corrosion pit

Data that has been collected from the trials site does not contain information on rail breaks and defectives. Therefore this report does not discuss them further. Work is being progressed in work package WP4.2 into identifying the causes and the actions required when broken and defective rails are found.

4. Data Processing

The data that has been collected over a number of years by the two rail manufactures have been stored in different locations related to the projects that the information has been gathered for. To allow data collection with the same variables and format a spreadsheet (int-sp4.1-ot-05-061129-d1-MonitoredSites) has been devised that has been used to collect all data. The two companies have used this spreadsheet in different ways therefore before any analysis of the data could be carried out some treatment of the data was required to make the data compatible.

4.1 Received Data

4.1.1 Corus

Site monitoring has been carried out at a number of locations around various European networks. Each monitored site has several test locations usually three but sometimes more with the same track geometry. A number of site visits have been carried out on different days with timescales ranging from 1-2 years to one site that was monitored over 11 years. Therefore the Corus database contains just under 2000 measurements. The degradation mechanisms monitored were wear for all sites, in the form of profile measurements and for some sites RCF measurements. The gauge and cant were also monitored that may allow degradation of track geometry to be estimated but no knowledge of maintenance procedures such as tamping is known. Each individual measurement has an identification number called a TID, those from Corus are numbered in the range 1 to 10,000.

To allow analysis of the data, the measurements have been aggregated together so that those with the same track identity, location, radius, rail grade, direction and project. This gives 85 individual sites with the number of measurements ranging from 3 to 105. The sites from Corus UK are numbered in the series 1-100. To enable the assessment of degradation as a function of cant, the mean of the measured values (rounded to nearest 5) has been used.

4.1.2 Voestalpine (VAS)

The data received from voestalpine contained 206 data measurements; a similar aggregation process was carried out using radius, rail grade and daily traffic (traffic wasn't used for the Corus data as it was found to be the same for each site). Test sites monitored by voestalpine with the respective railways are setup in a similar way to those of Corus. Each test site consists of at least three measurement points which were monitored on a regular basis twice a year. Since wear or RCF crack measurement was not generally performed by voestalpine employees or the railways themselves, the results have been manually extracted from reports. Preferably the latest available information and sometimes additional information from further measurement intervals, is given in the database. The given data are mean values of the measurements on the individual measurement points. Thus the 206 data sets describe 110 individual sites or design locations numbered in the range 101 to 300. The record identification number, TID, for data from voestalpine have all be numbered greater than 10000 to ensure traceability of data. The data received from VAS also contained calculations of the rate of wear and crack growth, using the maximum values and dividing by the total traffic.

4.2 Limitations of Data

To allow a comprehensive analysis of the data, account has to be taken of all possible variables that may affect the performance of rails in service. The data that has been collected has concentrated on the rails themselves with only key track geometry features, such as radius and cant being recorded. Even within the degradation mechanism there is a variability in the data that has been recorded due to the aims and nature of the projects, an example is wear and is discussed further in section 4.3.1.

One major limitation of the data is that the vast majority is for curves; there is only limited data available for tangent track or transition curves. This is because the major rail degradation mechanisms are much more prevalent on curves which have therefore been of more interest. Transitions have only been monitored as an add on to the monitoring of the associated curves, transitions contain more variables which make interpretation of results more difficult and therefore are not targeted separately for monitoring.

The key areas where information is lacking include:

- Track Layout and Geometry – The features recorded are normally limited to curvature and cant. Those lacking include:
 - The location of the site in relation to stations, switches & crossing and signals, which will have an effect on acceleration/braking of the trains and consequently the forces that the rail undergoes.
 - Longitudinal gradient, which again will affect the behaviour of the vehicle and the forces the rail undergoes.
 - Sleeper spacing. This is rarely recorded and therefore the standard design parameters used for each railway have been used, but the variability in actual to design is unknown.
- Traffic – The only data usually provided is an annual traffic figure (MGTPA – Million Gross Tonnes per annum). The type of traffic running on a test site affects the loading parameters and therefore the stresses that the rail is subjected to. Detailed information such as the following is often not available:
 - Accuracy. Often no details are provided on how the traffic figure has been calculated. Some traffic data is calculated from the working timetables which include all trains whether they run or not (freight trains in working timetables often do not run). Others can be calculated from the signalling system.
 - Type of traffic/vehicles. An important parameter as different vehicle types result in different contact stresses.
 - Wheel Profiles. Vehicles often have a design profile but this deteriorates in service and, therefore, a rail is subjected to many thousand of wheels with different profiles all resulting in a range of contact stresses.
 - Speed. The only readily available figure is maximum line speed. No breakdown is available of the speed of different vehicles (freight trains travel at much lower speeds than passenger trains on the same line), which will result in different contact stresses.
- Maintenance Activities. The maintenance of track is a key activity that affects the life of the rail.
 - Grinding is carried out to remove RCF cracks as well as to restore the profile of the rail. During site visits recent grinding is evident by the presence of residual grinding marks. What is often not known is the date of grinding or the magnitude of metal removal. Grinding is a minor problem as it can be taken into account during calculations, see section 4.3.1.
 - Tamping. To attain correct track geometry, tamping is carried out often during the site monitoring. It can therefore affect the cant and hence the curving properties of the vehicles. Unfortunately it is rare that information on tamping is passed to those carrying out the site monitoring hence its effect on the results is unknown.
 - Lubrication. The lubrication of curves is a common feature to lower the wear by reducing the friction coefficient and hence traction forces. Unfortunately even where a lubricator is noted as being present the effectiveness is hard to quantify. Measurement of the friction coefficient can be made using devices such as Tribometers but this is only for the rail at one moment in time, the action of wheels and metrological conditions will alter the friction coefficient to a large extent.
- Meteorological Conditions.
 - The effect of the variability of the weather on the performance of rail in service is an unknown that has to be accepted. The lubricating affect of rain on the wheel contact has a major affect on the friction coefficient and hence on the contact stresses between the rail and wheel. Only the installation of a weather station alongside a test site would give accurate information of the weather that the test rails are subjected.

It can be seen from the list above that all the variables, which are unknown for some or all test sites, have an effect on the contact stresses between the wheel and rail. This is important because the degradation of rail is

a result of the stresses arising from the contact of the wheel. All of the above will affect these stresses to a greater or lesser extent. Liaison with the infrastructure managers may allow some of the variables to be filled in although this will be difficult for some of the older test sites. Even so there are other variables that will remain unknown and are therefore part of the errors present in the derivation of rail degradation algorithms.

4.3 Combined Data

The calculations described in this section have been used to normalise the data for the different amounts of traffic that the monitored sites have encountered. The results allow graphs to be plotted to identify the trends in rail degradation, Section 4.3.

4.3.1 Wear Calculations

The wear of rail is measured by taking a profile with a device such as a Miniprof and comparing with a standard as rolled profile. It is characterised by several different parameters with the common measures being vertical, 45°, horizontal and the worn area. The first two parameters have been used by Corus for all their measurements with the second two not being reported. VAS in contrast has used all four parameters but those reported are different for each site due to the requirements of each project. To allow all site data to be used then a method of combining the individual wear measurements to give a total wear parameter is required. This is an area that still requires further work. At present, to give a statistical meaningful analysis, the measurements that have been used to study the wear of rail have been 45° and vertical wear of the high rail.

One important aspect with the wear data is the effect of grinding, which if not taken into account will result in a much higher wear rate than the true wear, similarly rerailling also has to be taken into account otherwise the wear would be too low. Therefore, where grinding or rerailling has occurred the wear has been reset to zero from the date of maintenance and the wear for subsequent inspections has been reported in terms of traffic from that date. All data has been normalised to one axis so the data from post grinding are included in the initial results. Further work is required to see if the grinding of the rail sufficiently alters the profile to affect the contact conditions thereby resulting in a different wear rate.

With the Corus data containing many different measurements for each site then a method to calculate the wear rate is required, this has been carried out in two ways. One method is to use the linear regression analysis (available in the specialist data mining software, Clementine) to calculate a line of best fit. There will be no wear with zero traffic therefore the intercept for the equation is set at zero.

Figure 5 shows the results for Site 41, a curve with a radius of 3000m. The equation for the line is:

$$\begin{aligned} 45^\circ \text{ Wear (mm)} &= 0.03076 \times \text{Traffic (MGT)} \quad R^2 = 0.967 & (1) \\ \text{Vertical Wear (mm)} &= 0.02166 \times \text{Traffic (MGT)} \quad R^2 = 0.907 & (2) \end{aligned}$$

Figure 5 demonstrates that the wear may not be linear to improve accuracy a polynomial could be fitted to this data, unfortunately the other test sites do not give such a good relationship. To allow comparison and also to simplify the degradation algorithms polynomial regression has not been used. It should also be emphasized that the rate of wear can be affected by climatic/weather conditions and hence the rate may deviate from linear over a long period. A second method of calculating wear using the maximum values has been carried out. All data points with greater than 75% of the maximum traffic for each site has been averaged, see Figure 6. The mean wear is then divided by the mean traffic to give a gradient of a straight

line, with a constant of zero this is equivalent to a wear rate.

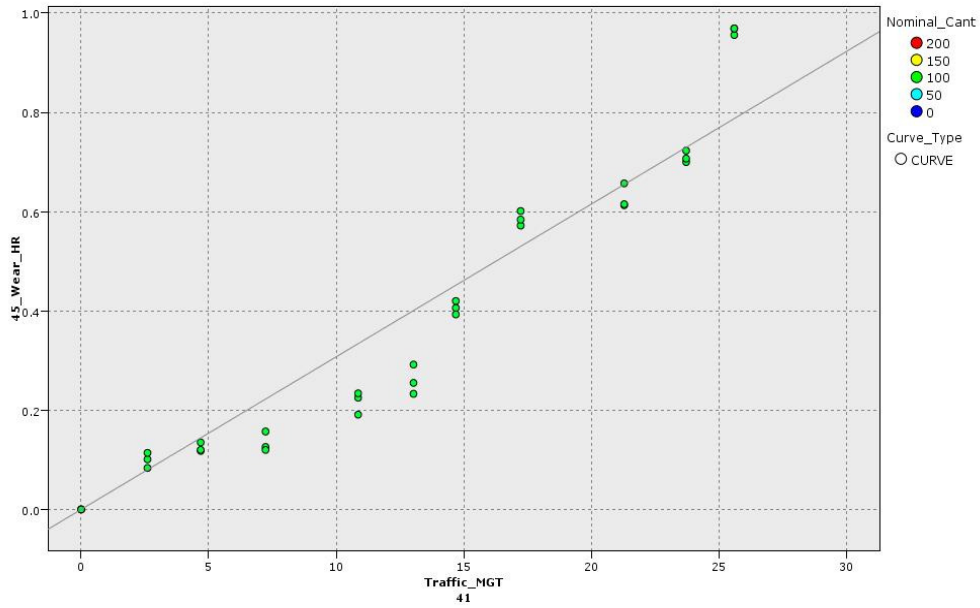


Figure 5 – 45° Wear against traffic – Regression Analysis

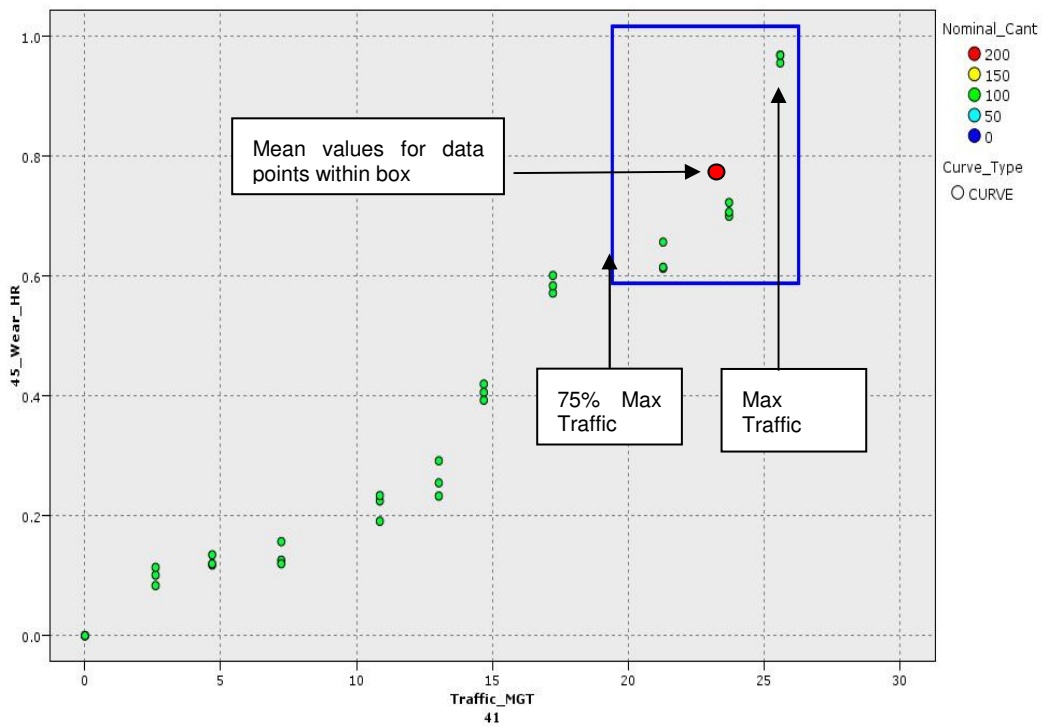


Figure 6 – 45° Wear against traffic – Maximum Wear Rate Analysis

For the same site as above:

$$45^\circ \text{ Wear (mm)} = 0.0326 \times \text{Traffic (MGT)} \quad (3)$$

$$\text{Vertical Wear (mm)} = 0.0249 \times \text{Traffic (MGT)} \quad (4)$$

The data for horizontal wear and worn area have been treated in a similar way.

4.3.2 Rolling Contact Fatigue (RCF) Calculations

The data on rolling contact fatigue from site monitoring is much more sparse than wear data. The two parameters that have been measured are the surface crack length measured using a ruler and the crack depth which has been measured by either ultrasonic or alternating current potential drop (ACPD) equipment. The data also allows the calculation of the interval from installation of the rail until the cracks become visible, this is known as the period to initiation. To allow some quantification of the tendency for sites to produce rolling contact fatigue, the following calculations on the growth of cracks with traffic have been carried out for both surface crack length and crack depth.

Several different measurements of crack growth have been carried out; the equations given below are for surface crack length with similar equations used for crack depth. To calculate the growth of cracks during the monitored period equation 5 has been used for all sites.

$$\frac{\text{Maximum Crack Length/Depth} - \text{Minimum Crack Length/Depth}}{\text{Maximum Traffic or Traffic from initiation of cracks}} \quad (5)$$

Where maximum traffic is calculated by the number of days from the first site date to the final inspection date multiplied by the daily traffic.

It is also possible to measure the rate of crack growth since the rail was installed using equation 6.

$$\frac{\text{Maximum Crack Length/Depth}}{\text{Total Traffic}} \quad (6)$$

Where total traffic is the number of days since installation to the date of the maximum crack length multiplied by the daily traffic in tonnes. For the voestalpine data in the vast majority of cases the results are identical to equation 5, the only difference being where the rails have been ground.

The calculated growth rate since installation includes the period required for crack initiation (PTI), it is therefore not a true growth rate but a measure of RCF damage. Figure 7 demonstrates how the period to initiation affects the crack growth rates. The period to initiation can also be an important parameter in terms of characterising RCF life as it allows an estimation of the vulnerability of rail to initiate RCF.

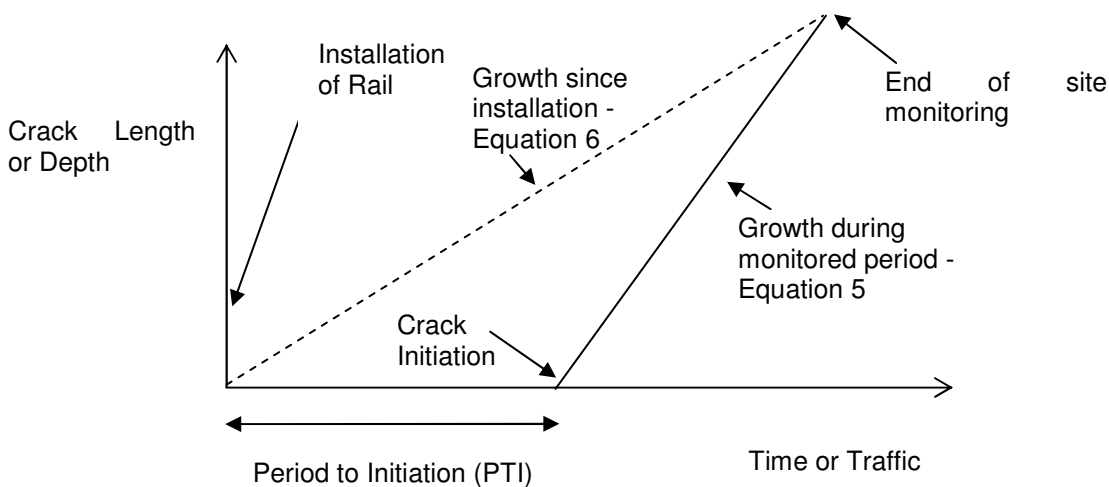


Figure 7 - Schematic of crack growth rates

5. Rail Degradation

The following graphs demonstrate the initial analysis of rail degradation identifying the trends that require more detailed investigation.

5.1 Wear

Analysis has been carried out to investigate what factors effect the wear of the rail using both the vertical and 45° measurements of wear for the high or outer rail in curves. These are the two measures of wear for which the database contains the greatest amount of data.

The 45° wear rate (in mm/100MGT) is plotted in Figure 8 for grade 220 rail and Figure 9 for other rail grades against radius (in metres). The majority of the data is for grade 220 rail steel which includes equivalent rail steels made before EN13674-1 came into affect, such as UIC800 and BS11 normal grade. The other rail grades have also been grouped together with the modern name used in the graphs.

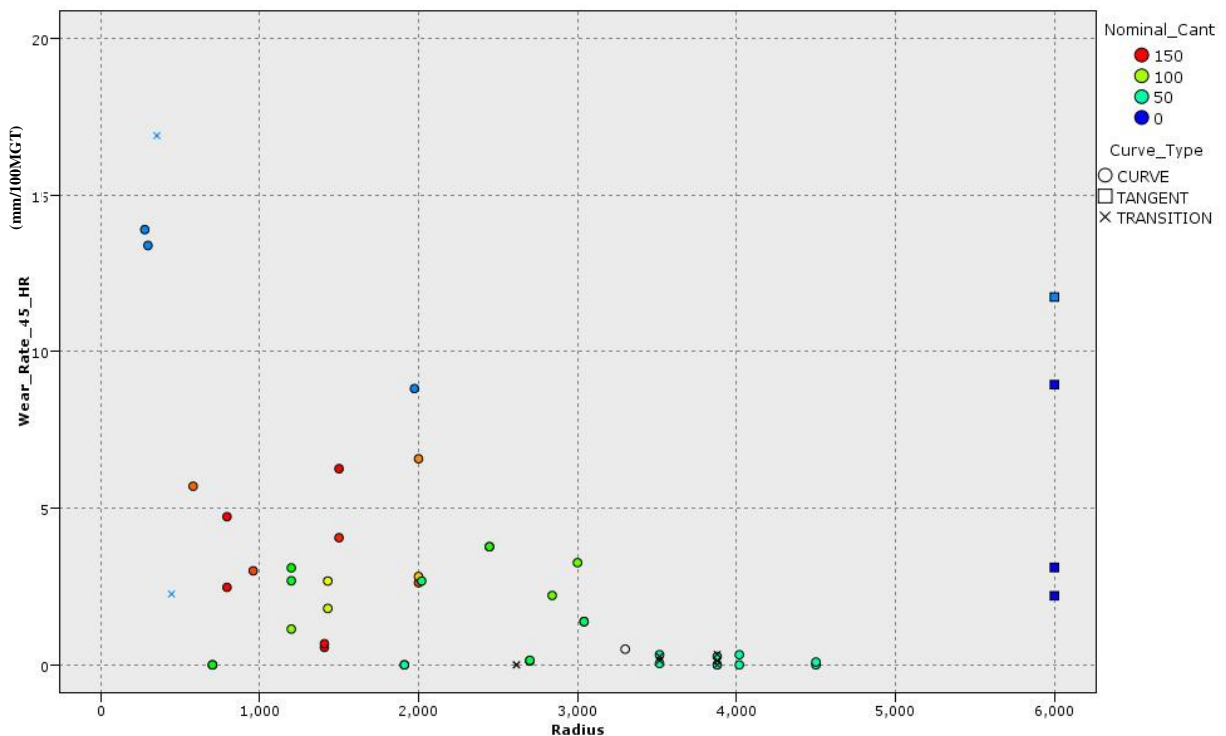


Figure 8 – 45° Wear of grade 220 rails - nominal cant

The results for the 45° wear rate show that the highest wear is for small radius curves, with a general trend of decreasing wear with increasing radius, this is more pronounced for Figure 9 than for the grade 220 steels. An exception to this behaviour are the results for tangent track, which are much greater than those for the higher radius curves (>4000m). A possible explanation for this is that the tangent track, with one exception, is associated with curves i.e. it precedes or follows a curve., The exception test site exhibited the lowest wear. Therefore the vehicles traversing the majority of the tangent track test sites may demonstrate instability resulting in higher track forces and therefore high wear. . Two of the tangent test sites also have canted track which will also result in higher track forces. However, other factors such hunting movements or grinding to remove corrugations may have affected the results. Consequently, the current analysis demonstrates the need for accurate maintenance records to make track monitoring of degradation

meaningful. For all curve radii there is a considerable spread in the results, this is especially the case for curves with radii of between 1500m and 3000m for grade 220 rails. The reasons for this range are highlighted in section 4.2, but one factor that is possible to take into account is cant, which can be overlaid on to the graphs using different colours, Figure 8. This is nominal cant which is constant for each curve but the speed of vehicles is also important therefore cant deficiency, h_d , has been calculated using equation 7 (after Esveld[2]):

$$h_d = h_{id} - h = \frac{11.8V_{max}^2}{R} - h \quad (7)$$

where

- h_{id} = Ideal cant(mm)
- V_{max} = Line speed (kmh⁻¹)
- R = Radius
- h = Actual cant

Cant deficiency is overlaid on to the 45° wear of non grade 220 rail in Figure 9.

Taking into account the large spread in results, there is sufficient evidence that the grade 220 rail steels possess worse wear performance than the other grades. This can be seen in Figure 10 which is a plot of the hardness of rail against the wear for curves of radius less than 700m; the results confirm that there is decreasing wear with increasing hardness. Grade 220 rails demonstrate more than double the 45° wear for the tighter radius curves than harder grades. Interestingly, Figure 10 also demonstrates that R320Cr rails have a very similar performance to the harder heat treated rails for curves with a tighter radius.

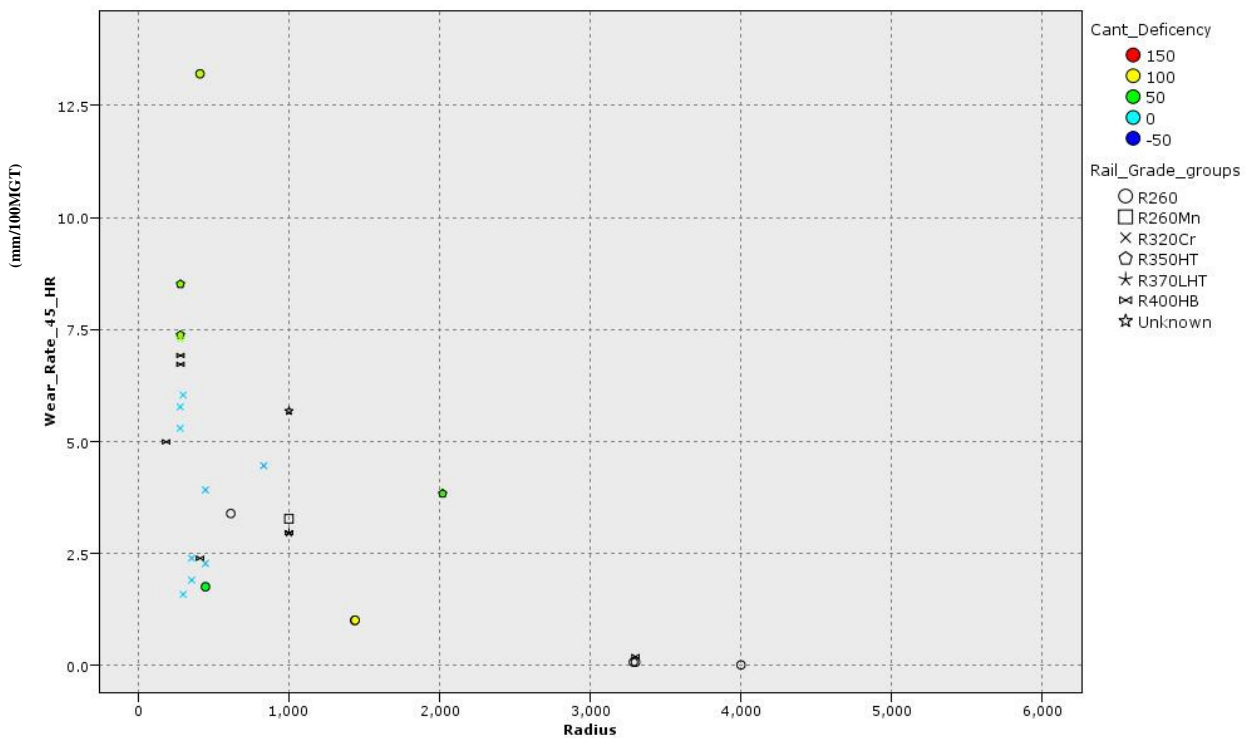


Figure 9 – 45° Wear of non-220 grade rails

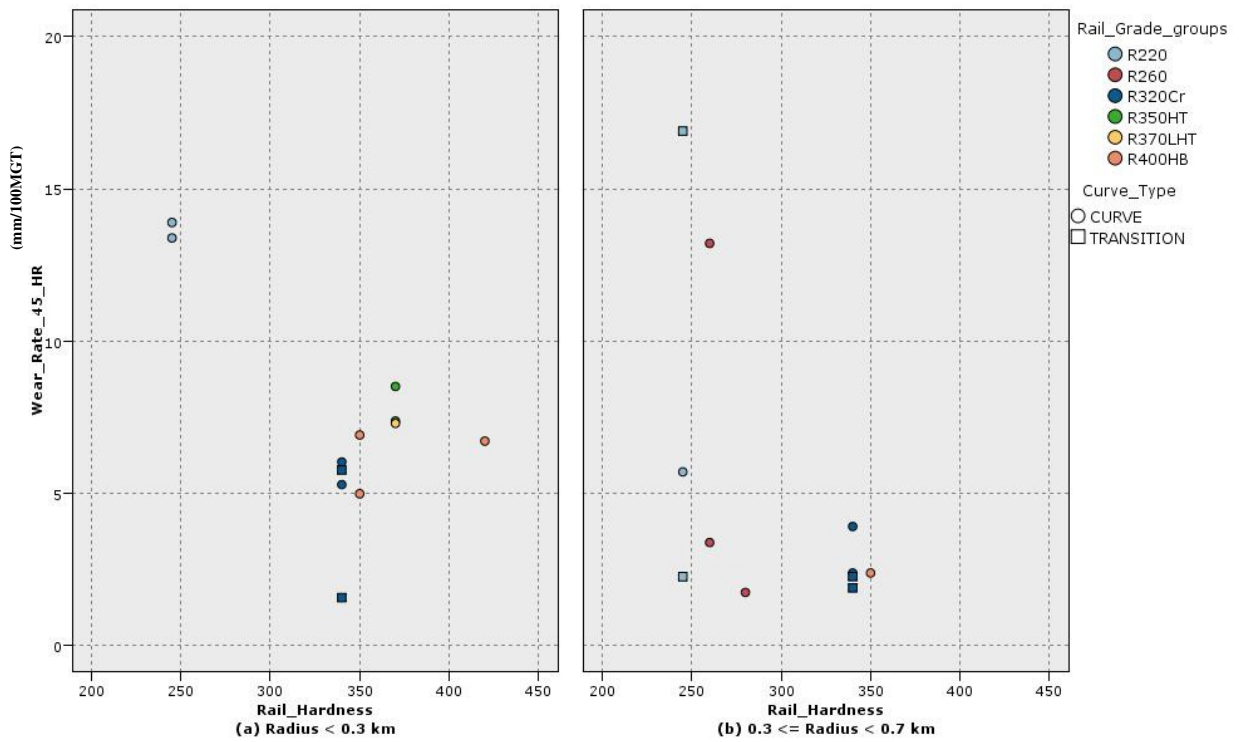


Figure 10 - Affect of rail hardness on 45° wear of curves with radius less than 700m

45° wear rate (radius); total load >45 Mio to

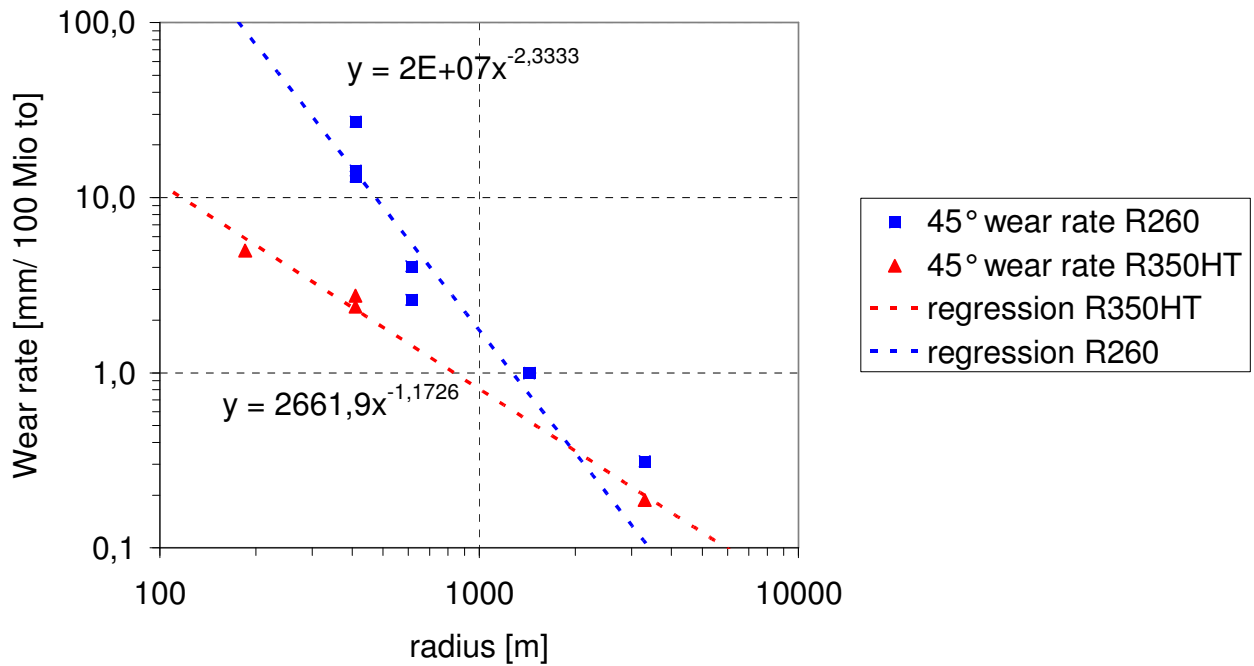


Figure 11 - log wear rate against log radius, R260 and R350HT

One way to simplify the plots and identify trends is by plotting different functions of the track parameters against the wear rate. Figure 11 is a plot of the logarithm of the radius against the logarithm of wear for grade R260 and R350HT rail. After installation of a new rail and initial grinding, a certain accumulated load is necessary to produce a continuous running band by wearing away the residual grinding marks. The wheel/rail contact tends to develop conformal conditions. In the early stages the wear rate shows a large amount of scatter. For this reason only measurements from site locations which have carried at least 45 million gross tonnes (MGT) have been selected to compare the wear behaviour of R260 with R350HT in Figure 11. The general trend of a higher wear resistance of the head hardened rail steel grade R350HT compared with the standard carbon grade R260 is obvious (The behaviour can be described by a power function given in the diagram). For sharp curves with greater wear the enhancement in wear resistance is greater than three. But the wear rate for the same radius may vary about two times, as shown for the grade R260 installed in the 400m radius curve. The reason for this variable behaviour is the difference in the time since installation with the longer period leading to a higher wear rate. This is not a general conclusion and is only relevant for this site. For curves with radius greater than 3000m it can be observed that there is no economic advantage of high strength pearlitic steels since grade R260 displays similar results with the variation lying within the accuracy of measurement and wear would not limit the rail life. Nevertheless the wear rate for R350HT in this curvature range is approximately half compared with grade R260. There is also a belief that harder premium grade steels are more corrugation resistant and consequently, one general conclusion that needs to be emphasized is that selection of rail grades should be based on the degradation mechanism operational at the site to be renewed. Since local track engineers are fully aware of the degradation mechanism that has curtailed the life of rail, grade selection based on degradation would be easier to implement.

Figure 12 shows the effect of cant deficiency on the wear for curves with different radii, it can be seen that only curves with a radius of 1000-1500m demonstrate a trend. Curves with greater radii demonstrate relatively low wear at the designed low cant deficiency but also show no trend. Since there is little or no spread in the cant deficiency for all sites outside the radius range of 1000 to 1500 m, it is not surprising that no trend of this parameter against wear is revealed by the analysis. For the sake of simplicity of the degradation algorithms, a similar dependency on the cant deficiency as shown for curves within the radius range of 1000-1500m has been assumed for the other curvature ranges too, although this is not expected to make any noticeable difference in the predicted levels of wear.

R220: wear rate 45° (cant deficiency); total load > 45 Mio to

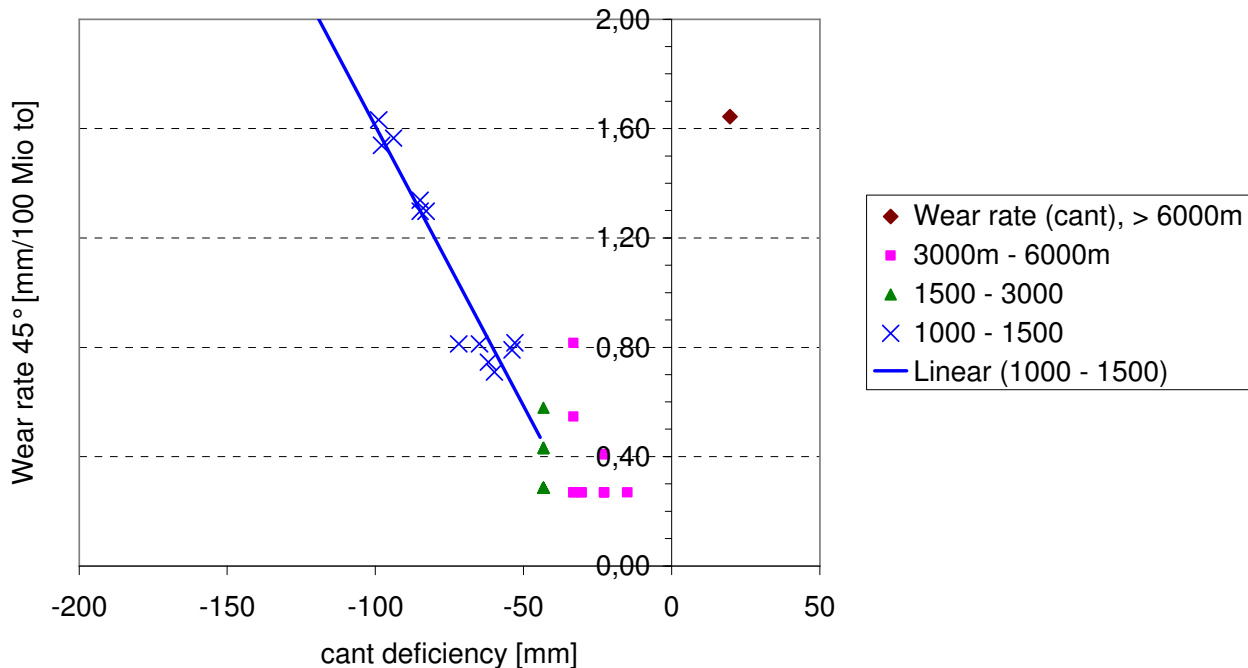


Figure 12 - Wear rate against log radius, 220

The results for vertical wear, Figure 13 and Figure 14, demonstrate that the wear rate near the crown of the head is much lower than near the gauge corner; for grade 220 rails it is 2 to 3 times lower. This is not surprising as in curves the contact stresses are higher at the gauge corner than on the crown of the rail [3]. There is also less of a trend with curvature for vertical wear than for 45° wear, for the 220 grade rails. In contrast the other rail grades show much higher vertical wear for the lower radius curves. The overlay of cant deficiency demonstrates that, like 45° wear, its effect is unclear on vertical wear. Although further information on the maintenance practices and traffic characteristics of the various monitored sites would be expected to improve the observed trend, the effort required to undertake such an analysis could not be justified. Instead, it emphasizes the need for such information to be gathered in future controlled track trials.

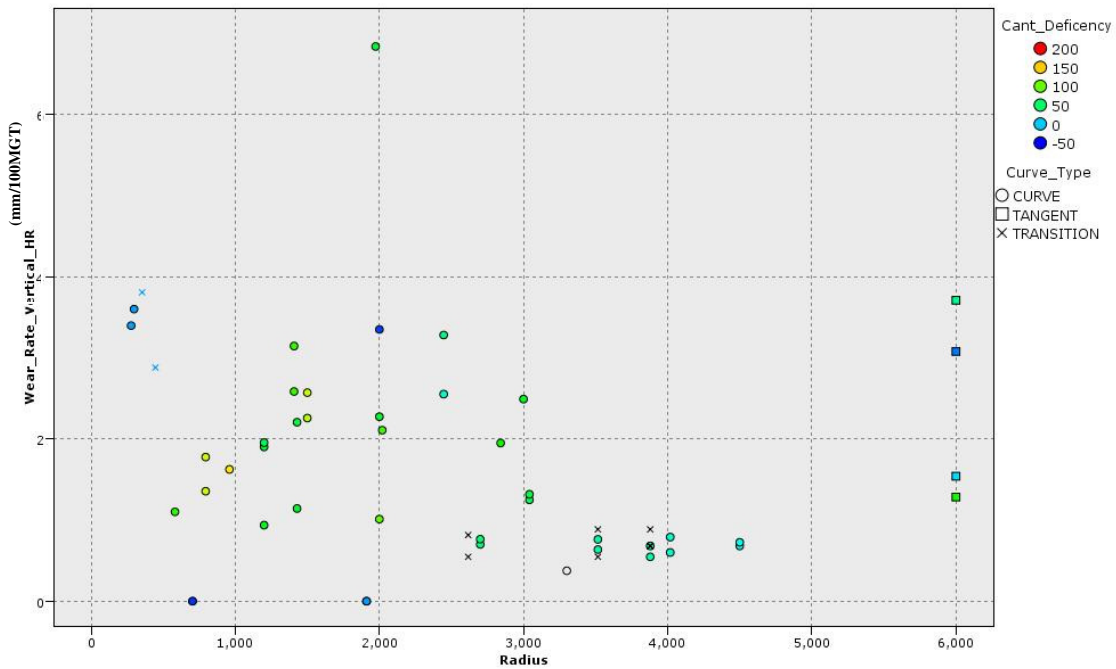


Figure 13 - Vertical wear of grade 220 rails – cant deficiency

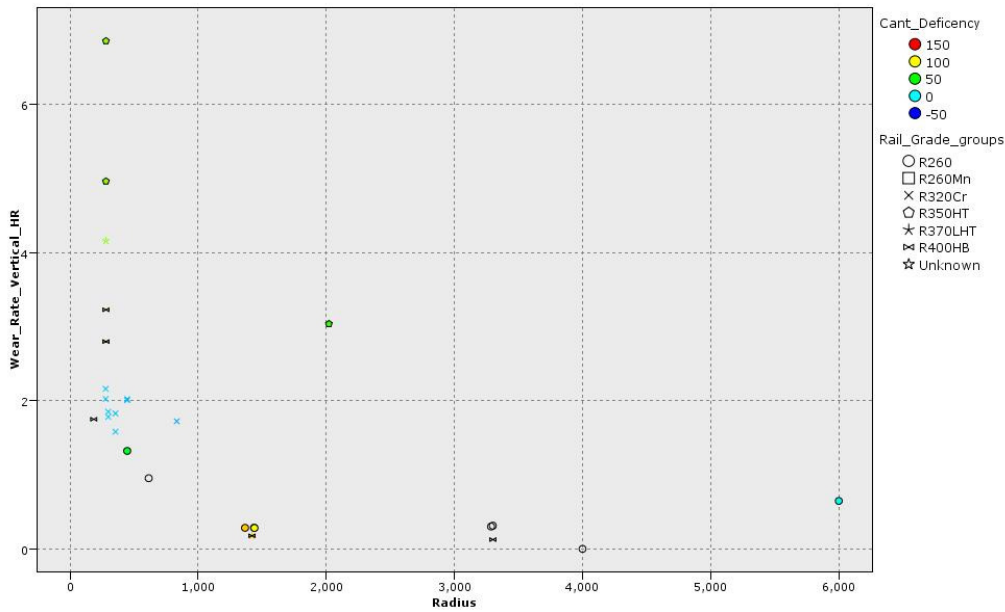


Figure 14 - Vertical wear of non 220 grade rails – cant deficiency

Y-axis needs units.

5.2 Rolling Contact Fatigue (RCF)

The calculations of RCF growth have been used to plot similar graphs to those for wear, Figure 15 and Figure 16. All four measures of crack growth are in units of mm per 100MGT. There is considerable difference in the magnitude of the crack growth measurements; those calculated from the date of installation are much lower than those during the monitoring period. The growth rate from the date of installation is not a true crack growth rate but includes the time to initiation plus the growth of the cracks once initiated. Of the two most important measurements of RCF cracks that reflect integrity of the rail is crack depth, although the easiest to monitor is surface crack length. It is therefore important to consider both when studying rail degradation.

The results from all four measures of crack growth demonstrate that rolling contact fatigue can be present on track with a wide range of radii between 500 and 4000m as well as tangent track. The tracks most likely to contain rolling contact fatigue are those with a radius between 500 and 3000m, with the highest rate of crack growth being for curves between 900 and 2000m. The results also confirm that grade 220 rails may be less resistant to RCF than harder grades which is in accordance with laboratory results. Other factors may also have an effect, especially the track characteristics and the behaviour of different vehicles.

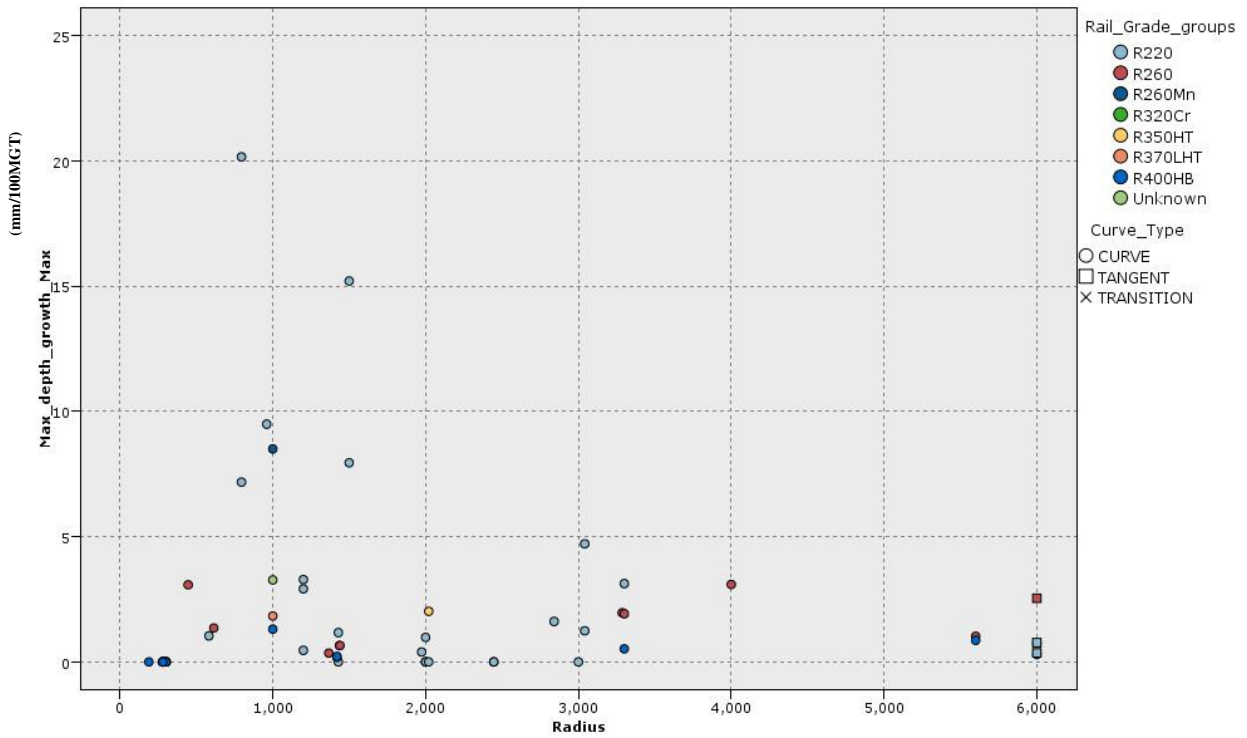


Figure 15 - Maximum crack depth growth rate since installation for all rail grades

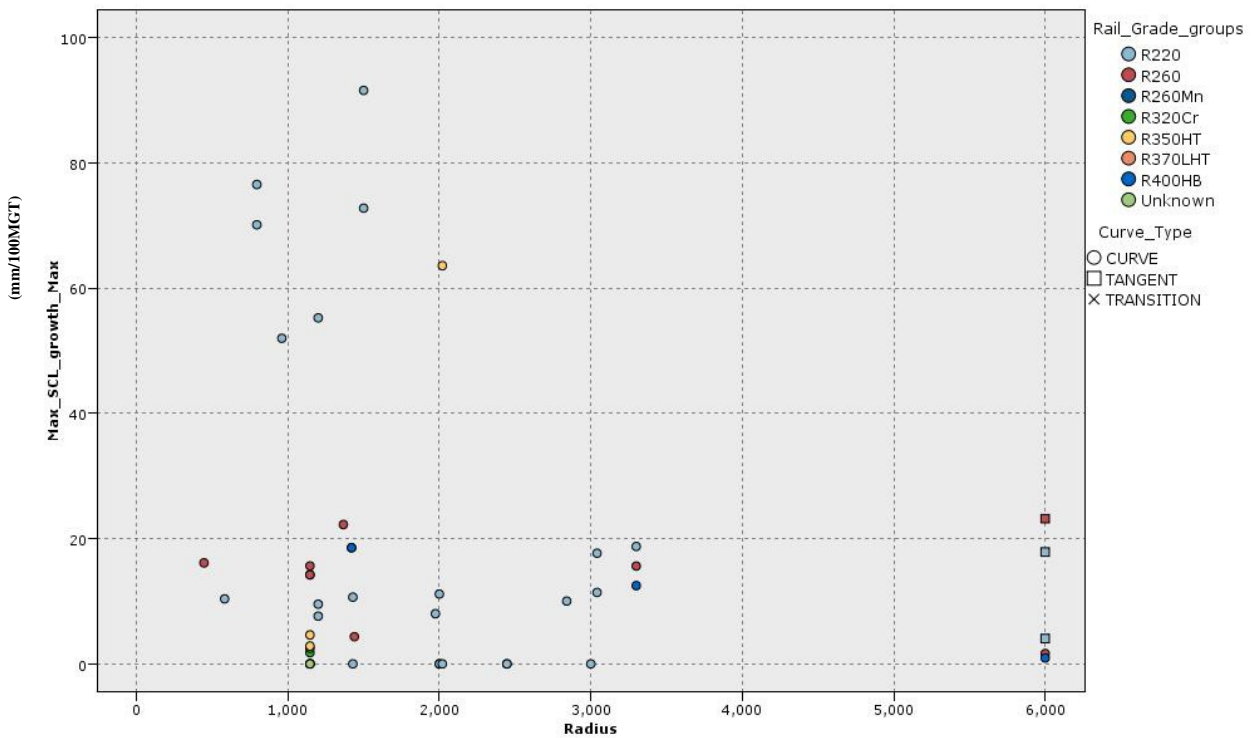


Figure 16 - Maximum surface crack length growth rate since installation for all rail grades

A study of the period to initiation of rolling contact fatigue defects has been carried out for grade 220 rails, some of which have been ground, Figure 16. In this graph, where the rail is classed as "RCF free" then the traffic is the total carried without RCF being present. The graph emphasises the finding highlighted above with a clear indication that RCF is most prevalent in curves with radii between 500 and 3000m and reveal the shortest time to initiation. The results also demonstrate that similar curves with the same radius show different degradation behaviours depending on the other parameters such as different vehicles as discussed above. Although based on very limited number of data points, the results reveal a shorter period to initiation on ground rails. This is somewhat surprising and further work is recommended to establish the influence of grinding on the subsequent period to initiation for the most commonly used rail grades.

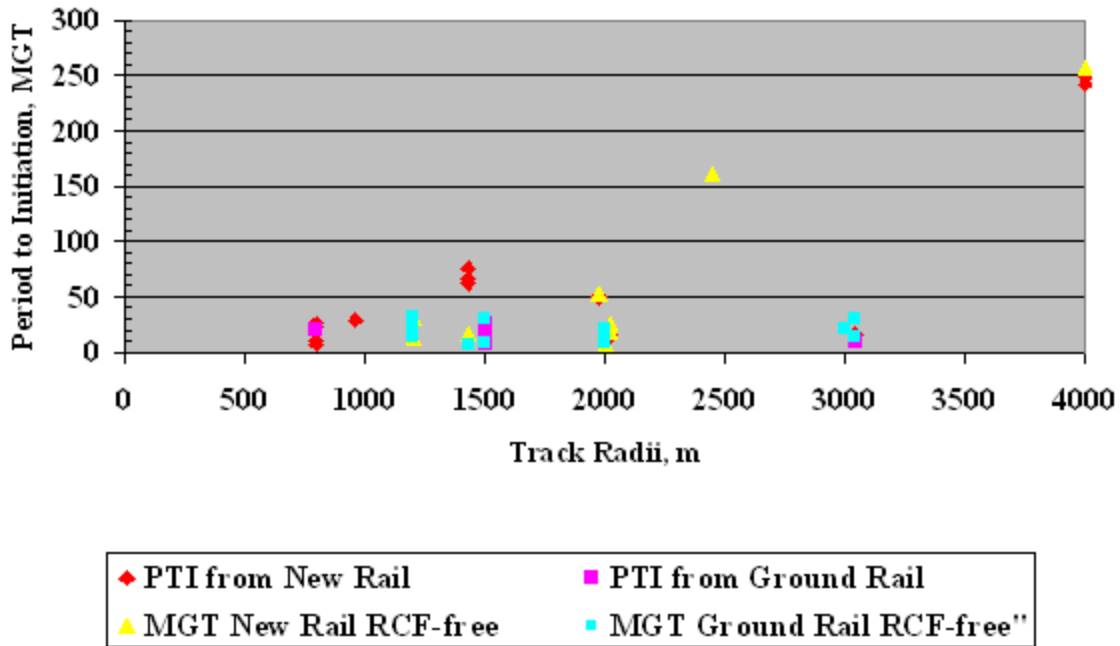


Figure 17 - Period to Initiation of RCF cracks

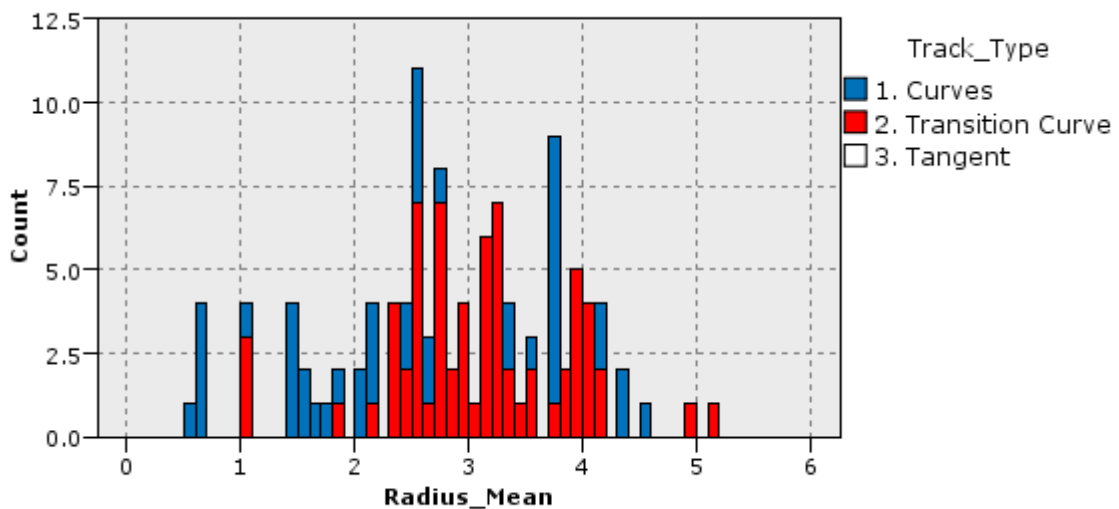


Figure 18 - Distribution of radius [1000m] for segmented track with RCF defects

The results from the segmentation exercise of track data, D1.2.5, for one of the IM's has been compared with the database of defects present over 5 years for the same section of track. This has allowed the relation of defects to different track geometries. Figure 18 shows the distribution of RCF defects for the radius of curves, the results indicate that RCF is a problem that occurs over a radius range of 500 to 5000m, confirming the results of the site monitoring. The results also demonstrate that RCF appears to occur more frequently on transition curves than those with a constant radius. The results from the analysis of the site monitoring data will be validated by comparison of the results with defect data for the segmented track if made available by the infrastructure managers.

The initial data analysis has demonstrated that the relationships in the degradation data are complex with large scatter in the results and further work is required to fully understand rail degradation and be able to relate it to track geometry. However, the following section demonstrates that with appropriate data from the monitored sites, simple numerical models can be derived and highlights where further work is ongoing to develop an improved understanding of rail degradation.

6. A Basis for a General Degradation Approach

A general degradation approach is to describe rail degradation by mathematical formulas to relate the dependency of the most important track (including geometry), loading and surface conditions.

6.1 Motivation

To provide a scientific basis for the recommendation for the use of different rail grades, the degradation behaviour of these materials has to be well known for different loading conditions. The observations of site tests show a large spread in the results for wear and RCF for track with similar basic characteristics such as radius and rail grade. The data available at present does not allow a simple regression analysis to be used for the derivation of rail degradation algorithms.

Other factors to be taken into consideration when studying the rail degradation are the forces that the track has to withstand. Approaches in the past have included finite element models (FEM), Multi Body Simulation (MBS) or analytical methods to provide detailed results on the track forces, contact forces/stresses, slip, flash temperature, wear and others for local situations. These calculations require accurate input data and complex models that require significant amounts of calculation time (especially FEM calculations), hence it is not possible to perform real time calculations for a larger system.

For this reasons the following is an attempt made to describe the rail forces and resulting rail degradation by expressions which can be implemented in simple spread sheet calculations. The modelling group within SP1 is carrying out detailed modelling of the contact forces for a selection of site to validate this approach.

6.2 Basic Conventions

The calculation is based on pragmatic assumptions; e.g. steady state conditions are assumed. Thus effects like initial hardening, shakedown and the formation of a running band are considered as starting conditions but are not characteristic of the long term behaviour. The total damage, wear and rolling contact fatigue are defined as depth from the initial new rail surface. New starting condition is assumed to be identical for new rails with or without initial grinding or after subsequent grinding if cracks are completely removed. The conventions are sketched in Figure 19 and can be summarised:

- Damage (D) rises linearly
- Wear (W) and rolling contact fatigue (RCF) are competitive mechanisms
 - $D = \text{Max}(W, \text{RCF})$
 - RCF crack length = RCF - W, if $\text{RCF} \geq W$; RCF crack length = 0, if $\text{RCF} < W$ then Figure 18 is valid

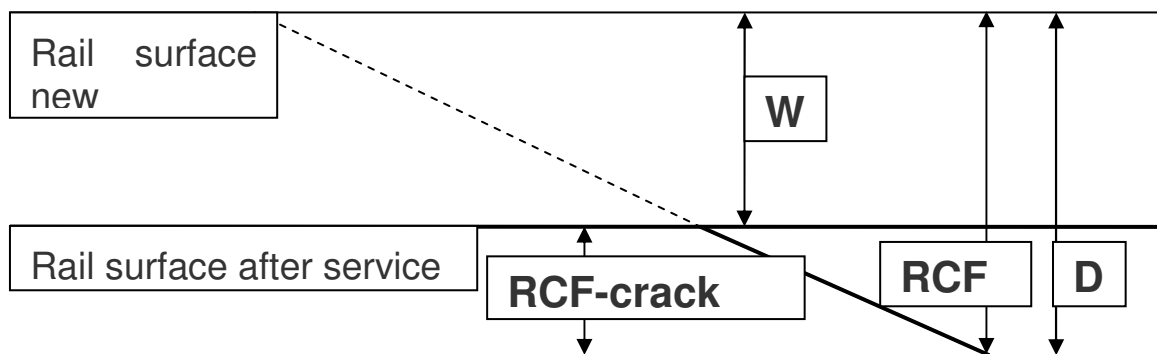


Figure 19 - Schematic of RCF and wear

6.3 Calculation

During the following sections several initial assumptions have been made which could be changed if later work was to show that a different assumption lead to a more precise prediction of rail degradation.

6.3.1 Input parameter

For the initial description of the track the radius, cant, rail grade, lubrication (considered by the maximum traction coefficient) and a qualitative characterisation of the track quality are chosen.

The vehicle is included in the calculation by its axle load, the centre of gravity, a minimum radius which can be passed without flange contact and the driven speed (at present the maximum track speed).

6.3.2 Resulting Loads

The radial horizontal load $F_{r,h}$ is calculated from the static axle load, a (kN), speed, V (m/s), and radius, r (m):

$$F_{r,h} = \frac{aV^2}{gr} \quad (8)$$

where $g = 9.81 \text{ m/s}^2$

A rail centred coordinate system (see Figure 20) has to be introduced. It has to be rotated around the longitudinal rail axes x by an angle α given by $\alpha = \arctan(C/W)$, with C (mm) = Cant and W (mm) = track width. The rail inclination is assumed to be 0. The resulting forces in the transformed coordinate system y and z are:

$$\begin{aligned} F_y &= F_{r,h} \cos(\alpha) - a \sin(\alpha) \\ F_z &= a \cos(\alpha) + F_{r,h} \sin(\alpha) \end{aligned} \quad (9)$$

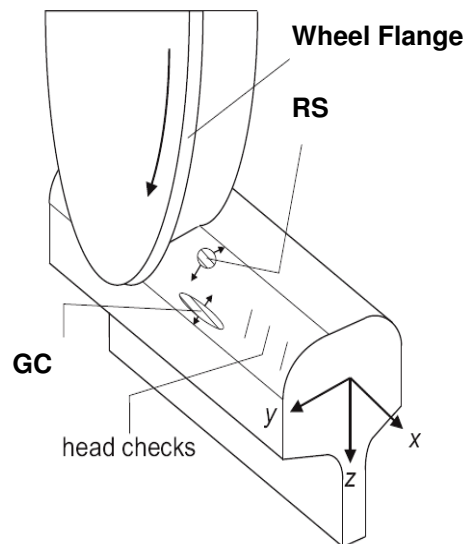


Figure 20 - Coordinate system for modelling

The radial component F_y is assumed to be completely carried by the high rail for wheel flange contact and is neglected for single contact at the surface. The loading in the z -direction follows, where HR = high rail and LR = low rail (where h = distance of the centre of gravity from the rail surface):

$$HR_z = \frac{\left(\frac{F_z W}{2} + F_y h\right)}{W} \quad (10)$$

$$LR_z = F_z - HR_z$$

The calculated loads will be greater due to bad track quality, simply considered by a factor ϕ :

- $\phi = 1.04$ for very good track quality
- $\phi = 1.08$ for good track quality
- $\phi = 1.12$ for bad track quality

The dynamic impact is considered by a dynamic coefficient γ (based on [4]):

$$\gamma = 1 + 0.5 \left(\frac{V - 60}{190} \right) \quad ; \text{ for } 60 < V \leq 300 \quad (11)$$

$$\gamma = 1 \quad ; \text{ for } V \leq 60 \quad (12)$$

6.3.3 Resulting stresses

Contact stress calculation is a non trivial task by simple spread sheet calculations since the contact conditions are statically indeterminate. Thus an estimation of the contact patch size and the resulting stresses must be performed. The equivalent von Mises stress for different traction coefficients are calculated for the elastic contact between cylinders according to the formulations of Smith and Liu [5]. The results for a maximum Hertzian contact pressure, P_0 , of 1000 MPa at various depths below the surface (given by a contact patch half width a) are stored in a spread sheet named "Table VM".

Since the contact patch half width a (and the corresponding half width b for elliptical contact patches) depends on the loads and the shape of the contacting bodies further simplifications are made.

With the following equations from Johnson [6]

$$\mu_R = \frac{F_R}{P} = \frac{2}{3\pi} \alpha \frac{a}{R} = \frac{4}{3\pi} \left[\frac{P}{\pi R E^*} \right]^{1/2} \quad (13)$$

$$P_0 = \left[\frac{P E^*}{\pi R} \right]^{1/2} \quad (14)$$

It follows after rearranging equation 13 in terms of a and substituting in equation 14:

$$a = 2R \sqrt{\left(P_0^2 / E^{*2} \right)} \quad (15)$$

where μ_R is the coefficient of friction, F_R the rolling resistance, P the normal load, α a loss factor, a the contact half wide, R the radius of the wheel, P_0 the maximum contact pressure and E^* is the combined modulus for the wheel and rail, equation 16.

$$E^* = \left\{ \left(1 - \nu_1^2\right) / E_1 + \left(1 - \nu_2^2\right) / E_2 \right\}^{-1} \quad (16)$$

For identical wheel and rail materials $E_1 = E_2 = 210000 \text{ N/mm}^2$ and $\nu_1 = \nu_2 = 0.3$.

For three dimensional wheel/rail contact the assumption of a line contact on an elastic half space is not valid but can be used for estimation of the centreline of a contact patch where the conditions are assumed to be similar. To enable an estimation of the contact stresses a virtual radius R^* is introduced. R^* reflects the curvature of both contact partners (Rail is flat in longitudinal direction and convex in transverse direction while the wheel is convex in longitudinal direction and concave in transversal direction) in the considered orientation.

Three cases are considered so far:

1. Single point contact at the running surface (RS): R^* assumed to be 330 mm for both orientations (circular contact patch)
2. Single point contact at the gauge corner (GC): R^* assumed to be 120 mm for both orientations (circular contact patch)
3. Two point contact: $R^* = 80 \text{ mm}$ at the gauge corner in transversal direction, $R^* = 400$ at the gauge corner in longitudinal direction, $R^* = 80 \text{ mm}$ in transversal direction

For these cases the normal load is calculated and stored in a spreadsheet named "Table Load". In which the normal load is calculated using $F_n = 2/3 P_0 \pi a^2$ for the circular contact patch and $F_n = 2/3 P_0 \pi ab$ for the elliptic contact patches.

The normal load for the three cases mentioned above is calculated as follows:

1. $F_{n,1} = HR_z$
2. $F_{n,2} = HR_z$

For single point contact near the gauge corner the contact force in the z-direction should be split in to normal and tangential components, which has not been done for simplification – for low angles between the z axis and the normal-direction the difference in the calculated equivalent stress should be reasonably low.

3. $F_{n,3,GK} = F_{n,3,RS} = 0,5 * HR_z$

The load is simply assumed to be half on each contact patch (see the discussion for $F_{n,2}$ above)

For single point contact, slip occurs only during stick/slip conditions or for general sliding of the wheel due to acceleration or braking. With the elastic model stick/slip conditions cannot be considered, so we assume a small amount of slip leading to a traction coefficient of $\mu = 0.05$ over the whole contact patch to consider traction forces at the surface. The traction force on the sliding contact patch will reach a maximum when the maximum friction coefficient is reached. The traction for single point contact mainly depends on the driving or braking forces (not yet considered) while for two point contact, traction forces also arise from constant slip due to the rolling radius difference. Thus the traction on the contact patches of two point contact is assumed to be the product of friction coefficient and the normal force on each contact location.

Using the above simplifications it is possible to calculate the maximum equivalent stress σ_{VM} for the three cases.

To calculate the stresses for the contact location the calculated normal forces are compared with the calculated normal loads in the lookup table "Table Load" for the assumed virtual R^* at the maximum contact pressure P_0 . The look up table will give the respective contact pressure P_0 that matches the normal load.

The maximum equivalent stress for the considered traction coefficient is selected from the table "Von Mises". Since the equivalent stress is stored in the table "Von Mises" only for a maximum pressure of 1000 MPa it has to be scaled by the proportion of the actual normal pressure divided by 1000.

6.3.4 Interpretation of interim results

The calculation developed so far has been coupled with the database reported in D4.1.1. The contact stresses for each included test site can now be quickly estimated. The maximum and minimum resulting equivalent stress σ_{VM} for the three considered cases can be interpreted to give a range of maximum stresses which may occur on the site for various running condition (Beside the assumption of wheel flange contact of the first axle for sharp curves, the 2nd or 3rd axle of the bogie will run on the high rail without flange contact).

The magnitude of the equivalent stress influences the fatigue behaviour of the rail surface. The greater the equivalent stress is with respect to the ultimate strength of the material, the more probable is (cyclic) plastic deformation at or below the rail surface. Consequently, there is a higher probability for the development of RCF and the rate of RCF crack growth rate is also likely to be higher if the initiating cracks are not worn away at an early stage.

Three selected results are shown in Table 1. For all sites the rail profile is BS113A, mixed traffic runs on the line and bad track quality and a maximum traction coefficient of 0.3 is assumed for these examples.

Site ID	Rail grade HR	Radius	Cant	Maximum Speed	Maximum Axle load	Depth_Crack_Growth_Rate	Single Point Contact RS	Single Point Contact GC	2 Point Contact GC	2 Point Contact RS	Min Vergl. SPG	Max Vergl. SPG	Tensile strength	Proportion $\sigma_{VM,max}/R_m$
		R	S	V _{max}	L _{max}		$\sigma_{VM,RS}$	$\sigma_{VM,GC,1P}$	$\sigma_{VM,GC,2P}$	$\sigma_{VM,RS,2P}$	$\sigma_{VM,min}$	$\sigma_{VM,max}$	R _m	-
-	-	m	mm	km/h	t	mm / 100 MGT	MPa	Mpa	MPa	MPa	MPa	MPa	MPa	-
34	R260	446	66	64	24	8,3	704	1387	1007	667	667	1387	900	1,5
12	R220	795	147	137	24	22,1	766	1510	1094	727	727	1510	700	2,2
41	R350HT	2020	75	161	24	1,5	766	1510	1094	727	727	1510	1280	1,2

Table 1 - Calculation of stresses for three test sites

If we compare the ratio of $\sigma_{VM,max}/R_m$ with the observed Depth Crack growth rate there is an obvious relationship. The higher this ratio, the greater is the increase in crack growth. However, it should be emphasized that there is still a large spread in this relationship. For example crack growth rate of less than 5mm/100 MGT can be found for $\sigma_{VM,max}/R_m$ greater than 2. The spread can be explained by the missing competitive degradation mechanism wear, which has not yet been included in the calculation, although there is also a belief that development of RCF cracks are strongly influenced by the coefficient of friction. In addition a process has to be implemented into the spreadsheet calculation to enable a more precise estimation of the actual loading conditions. A value of maximum equivalent stress greater than the ultimate tensile strength, R_m, would usually indicate failure of the material, but the estimated values are similar to those reported in the literature. For wheel/rail contact a number of arguments can be given to explain how rail steel can withstand such high contact stresses (by no means exhaustive):

- Cyclic hardening of the rail surface exceeds the monotonic strain hardening especially due to the development of beneficial residual stresses.
- Shakedown increasing the strength of the rail material
- For high strain rates the yield limit and tensile strength of metals increases
- The high hydrostatic pressure changes the material behaviour, but not the von Mises stress
- Wear leads to conformal contact conditions, so that the stresses on the surface may be over estimated

6.3.5 Intended further work

The approach to the calculation of rail degradation algorithms, described in this document is at an interim stage and more work remains ongoing to develop it further. The intended next steps can be summarised as follows:

1. A plausible relationship between the resulting external forces and the contact forces for the most probable contact position has to be defined. It would probably make sense to choose more than the three contact cases used at the moment.
 - a. The question of wheel flange contact for the leading wheel set can be considered by a minimum radius, which can be passed with free rolling.
 - b. Climbing of the wheel at the gauge corner would reduce the normal load at the running surface.
 - c. Track quality and dynamic impact has to be considered as they will not only increase forces but also increase the possibility of a local reduction of loading. Upper and lower boundaries of stresses have to be estimated to describe a spectrum of possible degradation mechanisms. This aspect of the development will utilise the work undertaken in WP 4.2.
2. For lines with different traffic or vehicles running on it, the relevant cases have to be considered with their proportion of passes.
3. For all those cases algorithms have to be defined to approximate not only the traction forces due to slip but also friction occurring on the contact surface (wear prediction).
4. When the description of contact conditions reaches a satisfying correlation compared with results from detailed modelling performed within SP1, degradation indices have to be defined.
 - a. Material behaviour has to be included into the algorithm.
 - b. Degradation indices have to be fitted to the observed degradation behaviour.

7. Conclusions

The degradation of rail is an important aspect in the safety and maintenance of railways. Therefore for a cost effective railway an understanding of the degradation of different rail grades is required. A more cost effective maintenance strategy, that would reduce life cycle costs, could be implemented if the rate of degradation was known as a function of track geometry and loading conditions. Therefore the aim of this report is to study data that has been collected over the last 30 years by the railways and rail manufactures to understand the wear and rolling contact fatigue of rail as a function of track and loading parameters. This is an interim report that details the initial findings; a final report will be produced after further data analysis has been carried out.

The initial results have demonstrated that wear and rolling contact fatigue can be related to the track geometry, especially the radius of curves. The analysis has demonstrated that this relationship is not simple and the results demonstrate considerable spread. The reason is the many different variables involved with railways and include the factors that have not been recorded during the site monitoring. The next steps are to carry out analysis of the data in more detail to allow an understanding of the reasons for the spread in results, part of this analysis will be to carry out simple contact stress modelling.

8. Bibliography

1. Jaiswal, S., *Rail metallurgy and the rail/wheel interface*, in: Wheel/rail Interface Management, Mayfair, London, 2003
2. Esveld, C., *Modern Railway Track*, MRT Productions, Duisburg, Germany, 1989
3. Clayton, P., *Predicting the wear of rails on curves from laboratory data*, *Wear* **181-183** pp11-19, 1995
4. Lichtenberger, B., *Handbuch Gleis – Unterbau, Oberbau, Instandhaltung, Wirtschaftlichkeit*, Tetzlaff Verlag, Hamburg 2004, 2. Auflage
5. Smith, J.O. and C.K. Liu., *Stresses due to tangential and normal loads on an elastic solid with application to some contact stress problems*. *J. Appl. Mech.*, **20**, pp157–166, 1953
6. Johnson, K. L., *The strength of surfaces in rolling contact*, *Proc. I.Mech.E.* **203**(2), pp151–163, 1989